J Bone Miner Metab (2008) 26:642–647
DOI 10.1007/s00774-008-0857-1

SHORT COMMUNICATION

Hiroaki Nakamura · Toru Hiraga · Tadashi Ninomiya
Akihiro Hosoya · Noboru Fujisaki · Toshiyuki Yoneda
Hidehiro Ozawa

Involvement of cell–cell and cell–matrix interactions in bone destruction induced by metastatic MDA-MB-231 human breast cancer cells in nude mice

Received: September 5, 2007 / Accepted: January 23, 2008

Abstract To clarify the mechanisms of bone destruction associated with bone metastases, we studied an animal model in which inoculation of MDA-MB-231 human breast cancer cells into the left cardiac ventricle of female nude mice causes osteolytic lesions in bone using morphological techniques. On the bone surfaces facing the metastatic tumor cells, there existed many tartrate-resistant acid phosphatase (TRAP)-positive multinucleated osteoclasts. TRAP-positive mononuclear osteoclast precursor cells were also observed in the tumor nests. Immunohistochemical studies showed that the cancer cells produced parathyroid hormone-related protein (PTHrP) but not receptor activator of NF-κB ligand (RANKL). Histochemical and immunohistochemical examinations demonstrated that alkaline phosphatase and RANKL-positive stromal cells were frequently adjacent to TRAP-positive osteoclast-like cells. Immunoelectron microscopic observation revealed that osteoclast-like cells were in contact with RANKL-positive stromal cells. MDA-MB-231 cells and osteoclast-like cells in the tumor nests showed CD44-positive reactivity on their plasma membranes. Hyaluronan (HA) and osteopontin (OPN), the ligands for CD44, were occasionally colocalized with CD44. These results suggest that tumor-producing osteoclastogenic factors, including PTHrP, upregulate RANKL expression in bone marrow stromal cells, which in turn stimulates the differentiation and activation of osteoclasts, leading to the progression of bone destruction in the bone metastases of MDA-MB-231 cells. Because the interactions between CD44 and its ligands, HA and OPN, have been shown to upregulate osteoclast differentiation and function, in addition to the cell–cell interactions mediated by RANK and RANKL, the cell–matrix interactions mediated by these molecules may also contribute to the progression of osteoclastic bone destruction.

Key words bone destruction · bone metastasis · breast cancer · osteoclast · bone marrow stromal cell

H. Nakamura (✉) · T. Hiraga · A. Hosoya
Department of Oral Histology, Matsumoto Dental University, 1780 Gobara Hirooka, Shiojiri, Nagano 399-0781, Japan
Tel.+81-263-51-2042; Fax+81-263-53-3456
e-mail: nakam@po.mdu.ac.jp

T. Ninomiya · H. Ozawa
Institute for Oral Science, Matsumoto Dental University, Nagano, Japan

N. Fujisaki
Graduate School of Oral Medicine, Matsumoto Dental University, Nagano, Japan

T. Yoneda
Department of Biochemistry, Osaka University Graduate School of Dentistry, Osaka, Japan

Introduction

Bone metastases are frequently associated with bone destruction [1,2]. Accumulating lines of evidence suggest that osteoclasts rather than cancer cells destroy bone in the pathophysiology of bone metastases [3,4]. Histological studies demonstrated that numerous osteoclasts are lining along the bone surfaces adjacent to metastatic cancer cells in bone metastases of several types of human cancers [4–7]. These findings suggest that enhanced formation and activation of osteoclasts induced by cancer colonization are critical to the establishment of bone metastases.

The interactions between receptor activator of NF-κB ligand (RANKL) expressed in bone marrow stromal cells and osteoblasts and RANK expressed in osteoclast precursor cells play an essential role in the differentiation of osteoclasts [8–11]. In osteolytic bone metastases, osteoclastogenic factors such as parathyroid hormone-related protein (PTHrP) produced by cancer cells have been suggested to upregulate the expression of RANKL in bone marrow stromal cells and osteoblasts, thereby accelerating bone destruction [1,2,12–15]. However, the morphological evidence to support this notion is poor.

In addition to the cell–cell interactions mediated by RANKL and RANK, cell–matrix interactions also play a role in osteoclast differentiation and function [16,17]. Among the many cell adhesion molecules (CAMs) that

connect cell and extracellular matrices, we focused on CD44, which is expressed in both osteoclast lineage cells [18] and several types of cancer cells [19] and possesses a varieties of biological functions in cancer metastasis and bone metabolism [20,21]. The CD44 ligands hyaluronan (HA) and osteopontin (OPN) are abundantly and widely distributed in the bone microenvironment [18]. Furthermore, CD44, HA, and OPN themselves, and their communications, have been shown to have positive effects on osteoclast differentiation and function [22–27]. Thus, we studied the localization of these molecules in bone metastases.

In the present study, we studied the mechanisms of bone destruction associated with bone metastases using a well-characterized animal model in which inoculation of MDA-MB-231 human breast cancer cells into the left cardiac ventricle of female nude mice causes osteolytic lesions in bone [5,7], using morphological techniques.

Materials and methods

Reagents

Antibodies against PTHrP and RANKL were purchased from Immunodiagnostic Systems (Bolton, UK) and Santa Cruz Biotechnology (Santa Cruz, CA, USA), respectively. Anti-CD44 polyclonal antibody was described previously [28]. Antimouse CD44 monoclonal antibody was purchased from BD Biosciences (San Jose, CA, USA). Anti-OPN antibody was kindly provided by Dr. Fukae (Tsurumi Dental University, Kanagawa, Japan). Biotinylated hyaluronic-acid-binding protein (HABP) was from Seikagaku Biobusiness Corporation (Tokyo, Japan). All other chemicals used in this study were purchased from Sigma-Aldrich (St. Louis, MO, USA) or Wako Pure Chemical Industries (Osaka, Japan) unless otherwise described.

Cell culture

The human breast cancer cell line MDA-MB-231 (American Type Culture Collection, Rockville, MD, USA) was cultured in Dulbecco's modified Eagle's medium (DMEM; Sigma-Aldrich) supplemented with 10% fetal bovine serum (FBS; Asahi Glass Techno, Tokyo, Japan) and 100 µg/ml kanamycin sulfate (Meiji Seika, Tokyo, Japan) in a humidified atmosphere of 5% CO_2 in air.

Reverse transcription-polymerase chain reaction (RT-PCR)

Total RNA was isolated using TRI Reagent (Sigma-Aldrich), and single-strand cDNA was synthesized using BD PowerScript Reverse Transcriptase (BD Biosciences, San Jose, CA, USA). The primer sets used for PCR were follows: human RANKL, ACCAGCATCAAAATCCCA AG/CCCCAAAGTATGTTGCATCC; human PTHrP, CAAGATTTACGGCGACGATT/GGGCTTGCCTTTC TTTTTCT. PCR was carried out using a thermal cycler (GeneAmp PCR System 9700; Applied Biosystems Japan, Tokyo, Japan). PCR products were separated on 2% agarose gels containing ethidium bromide and visualized under UV light. The size of the fragments was confirmed by reference to a 100-bp DNA ladder.

Animal experiments

Mice. Four-week-old female athymic nude mice (Japan SLC, Shizuoka, Japan) were used. All procedures for animal care were approved by the Animal Management Committee of Matsumoto Dental University.

Bone metastasis. MDA-MB-231 cells (1×10^5 cells) suspended in 0.1 ml phosphate-buffered saline (PBS) were injected with a 27-gauge needle into the left cardiac ventricle of nude mice under anesthesia with sodium pentobarbital (0.05 mg/g body weight; Dainippon Sumitomo Pharma, Osaka, Japan) as described previously [5]. Mice were killed at 1, 2, 3, and 4 weeks after injection.

Tissue preparation

Mice were anesthetized with sodium pentobarbital and perfused though the left ventricle with 4% paraformaldehyde and 0.1% glutaraldehyde in 0.05 M phosphate buffer (pH 7.3). Bouin's fixative was used for the immunohistochemical detection of RANKL and PTHrP. Tibiae were dissected, immersed in perfusion fixative for 2 h at 4°C, and then decalcified in 5% ethylenediaminetetraacetic acid (pH 7.3) for 10 days at 4°C.

Light microscopy

Specimens were dehydrated in graded ethanol, embedded in paraffin, and cut into 5-µm-thick sections.

Enzyme histochemistry. For tartrate-resistant acid phosphatase (TRAP) activity, dewaxed sections were incubated in a mixture of 3 mg naphthol AS-BI phosphate, 18 mg fast red violet LB salt, and 50 mM L-(+)-tartaric acid diluted in 30 ml sodium acetate buffer (pH 5.0) for 30 min at 37°C. For alkaline phosphatase (ALP) activity, sections were incubated in 0.1 M Tris-HCl buffer (pH 9.5) containing NBT/BCIP stock solution (Roche Diagnostics, Tokyo, Japan) for 1 h at 37°C. The sections were counterstained with methyl green.

Immunohistochemistry for PTHrP and RANKL. Sections were immersed in PBS containing 10% bovine serum albumin (BSA) for 15 min, and incubated with anti-PTHrP antibody (1:50 dilution) or anti-RANKL antibody (1:200 dilution) for 12 h at 4°C. They were finally incubated in Histofine Simple Stain mouse MAX-PO (Nichirei, Tokyo, Japan) or horseradish peroxidase-conjugated anti-goat IgG

(Santa Cruz Biotechnologies; 1:200 dilution) for 1 h at room temperature. After washing with PBS, immunoreactivity was visualized by immersion in a DAB-H_2O_2 solution (0.05% diaminobenzidine and 0.01% H_2O_2 in 0.05 M Tris-HCl buffer, pH 7.6) for 5 min at room temperature. The sections were then stained with hematoxylin.

Double fluorescent staining. For detection of CD44 and hyaluronan (HA), paraffin sections were incubated with anti-CD44 antibody (1:500 dilution) and biotinylated hyaluronic acid-binding protein (2 µg/ml) for 12 h at 4°C. They were immersed in Alexa-Fluor-594-conjugated antirabbit IgG (Molecular Probes, Eugene, OR, USA) containing Alexa-Fluor-488-conjugated streptavidin (1:200 dilution; Molecular Probes). For detection of CD44 and OPN, sections were incubated with anti-CD44 and anti-OPN antibodies (1:500 dilution each) for 12 h at 4°C. They were immersed in Alexa-Fluor-594-conjugated antirat IgG and Alexa-Fluor-488-conjugated antirabbit IgG (1:200 dilution; Molecular Probes). Fluorescence of specimens was observed under a fluorescence microscope (Axioplan 2; Carl Zeiss, Oberkochen, Germany) with the appropriate filter combinations.

Immunoelectron microscopy

Sections approximately 50 µm thick were cut using a vibrating blade microtome (VT1000S; Leica Microsystems, Tokyo, Japan). These sections were incubated in anti-RANKL antibody for 24 h at 4°C, followed by incubation with HRP-conjugated antigoat IgG for 24 h at 4°C. Immunoreactivity was visualized by immersion in DAB-H_2O_2 solution. After postfixation with 1% OsO_4 in 0.1 M phosphate buffer (pH 7.4) for 1 h at 4°C, the tissue slices were dehydrated in

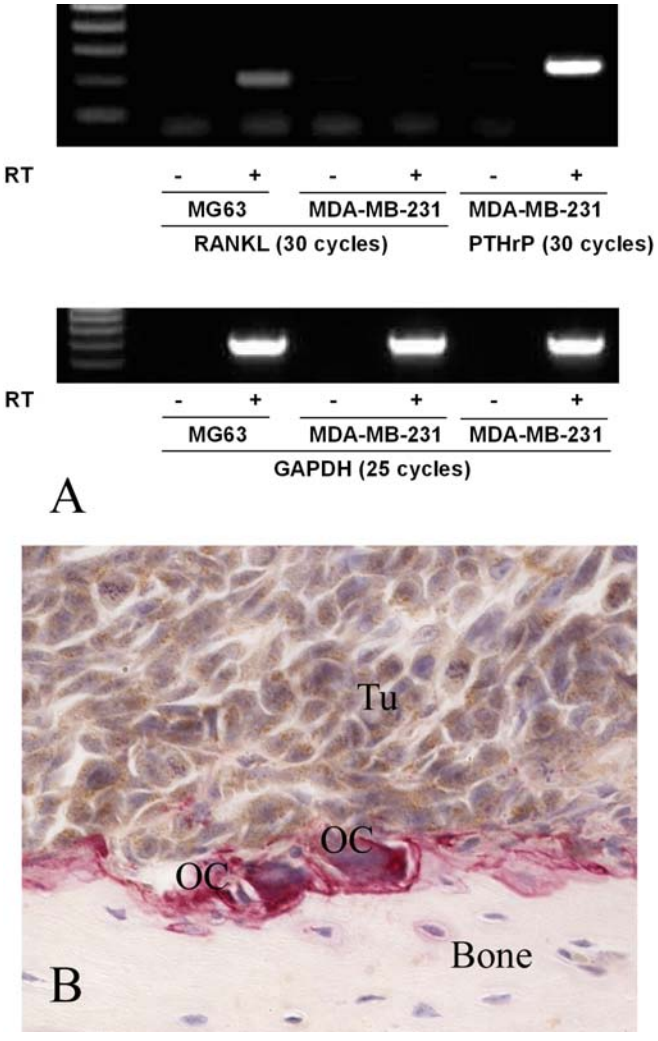

Fig. 1. Expression of osteoclastogenic cytokines by MDA-MB-231 cells. **A** Reverse transcription-polymerase chain reaction (RT-PCR) analysis of receptor activator of NF-κB ligand (RANKL) and parathyroid hormone-related protein (PTHrP) mRNA expression in MDA-MB-231 cells. **B** Immunohistochemical examination of PTHrP in bone metastases of MDA-MB-231. Most of the cancer cells (*Tu*) are positive (stained *brown*) for PTHrP. *OC*, tartrate-resistant acid phosphatase (TRAP)-positive osteoclasts; *Bone*, bone matrix. ×400

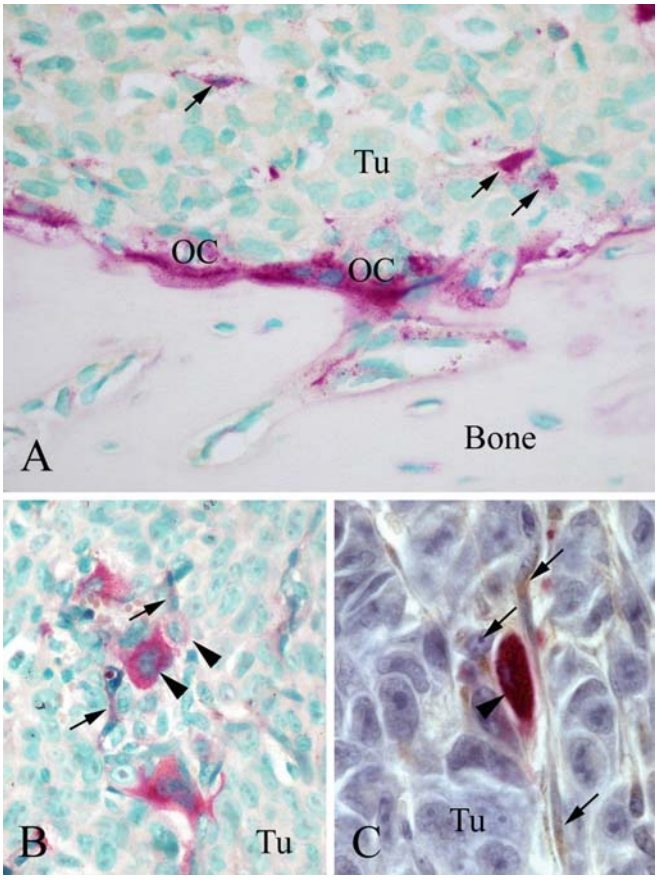

Fig. 2. Light micrographs of bone metastases of MDA-MB-231 cells. **A** Representative histological view of bone metastases of MDA-MB-231 cells. TRAP-positive (stained *red*) multinucleated osteoclasts (*OC*) are lining along the bone surface. TRAP-positive mononuclear cells (*arrows*) are also seen in tumor nests. TRAP staining: *Tu*, tumor cells; *Bone*, bone matrix. ×400. **B** Alkaline phosphatase (ALP)-positive stromal cells (*arrows*) are adjacent to TRAP-positive mono- and multinuclear cells (*arrowheads*). TRAP and ALP staining. *Tu*, tumor cells. ×300. **C** Immunolocalization of RANKL in a tumor nest. Some of the stromal cells are RANKL positive (stained *brown*), and they are in contact with a TRAP-positive cell (*arrowhead*). TRAP and immunohistochemical staining for RANKL. *Tu*, tumor cells. ×1000

graded acetone and embedded in Epon 812 (TAAB Laboratories Equipment, Berkshire, UK). Ultrathin sections were cut using an ultramicrotome (Ultracut UCT; Leica Microsystems) and stained with lead citrate. These sections were observed under a transmission electron microscope (H-7600; Hitachi High-Technologies, Tokyo, Japan) at an accelerating voltage of 80 kV.

Results

Production of osteoclastogenic cytokines by MDA-MB-231 cells in bone

Consistent with previous reports [13,14], RT-PCR analysis confirmed that MDA-MB-231 cells expressed mRNA of PTHrP but not RANKL (Fig. 1A). Immunohistochemical examination also showed that the metastatic MDA-MB-231 cells in bone produced PTHrP (Fig. 1B), whereas RANKL expression was not detected (Fig. 2C)

Interactions between bone marrow stromal cells and osteoclast precursor cells in bone metastases

In the bone metastases of MDA-MB-231 cells, numerous TRAP-positive multinucleated osteoclasts were observed along the bone surfaces (Fig. 2A). A number of TRAP-positive mono- and multinucleated round-shaped cells, putative osteoclast precursor cells, were also seen in the tumor nests apart from the bone surfaces (Fig. 2A). Double staining of TRAP and ALP demonstrated that ALP-positive spindle-shaped stromal cells were frequently adjacent to TRAP-positive mononuclear cells (Fig. 2B). RANKL immunoreactivity was detected in some of the stromal cells but not in the tumor cells. Double staining of TRAP and RANKL showed the contact between TRAP-positive mononuclear cells and RANKL-positive stromal cells (Fig. 2C). Immunoelectron microscopy further confirmed that RANKL was expressed on the plasma membranes of the stromal cells, and that they were in direct contact with osteoclast-like cells (Fig. 3).

Localization of CD44, HA, and OPN in bone metastases

We then examined the localization of the CAM CD44 and its ligands, HA and OPN, in the bone metastases of MDA-MB-231. Immunohistochemical examination showed that CD44 was expressed on the plasma membranes of MDA-MB-231 cells and multinucleated osteoclast-like cells (Fig. 4A). HA was widely distributed in the tumor nests (Fig. 4B). Colocalization of CD44 and HA was frequently found in the contact regions between cancer cells and osteoclast-like cells (Fig. 4C). Immunoreactivity of OPN was detected in several MDA-MB-231 cells and extracellular matrices in the tumor nests as well as in bone matrix (Fig. 5B). Colocalization of CD44 and OPN was occasionally detected around MDA-MB-231 cells (Fig. 5C).

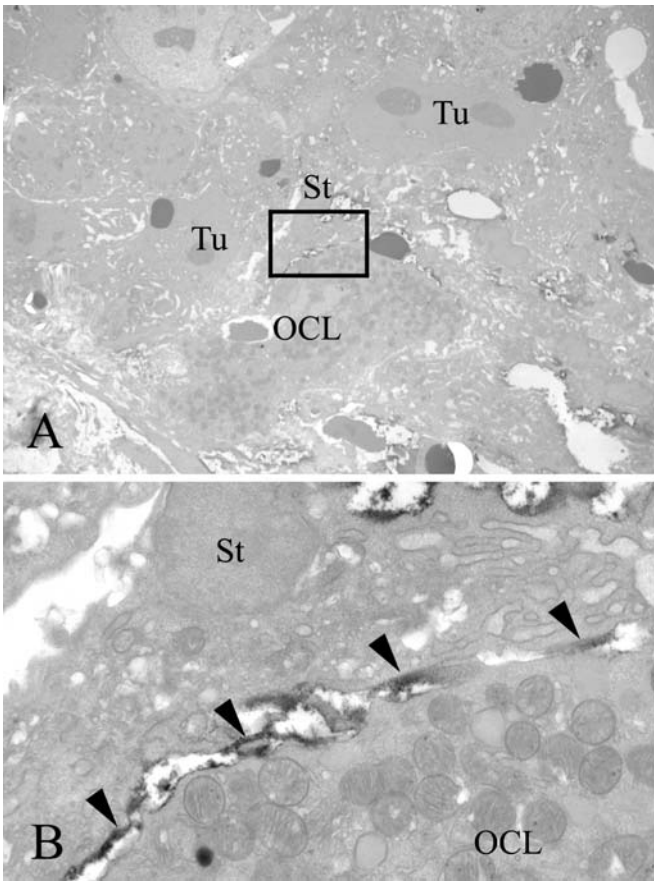

Fig. 3. Immunoelectron micrographs indicating localization of RANKL. **A** Tumor cells (*Tu*), a stromal cell (*St*), and an osteoclast-like cell (*OCL*) are seen in a tumor nest. ×2000. **B** Higher magnification of *outlined area* in **A**. Immunolabeling (*arrowheads*, stained *black*) is detected on the plasma membrane of the stromal cell (*St*) in direct contact with the osteoclast-like cell (*OCL*). ×6000

Discussion

Our histological studies show that numerous TRAP-positive osteoclasts existed on the scallop-shaped bone surfaces facing the metastatic MDA-MB-231 human breast cancer cells. We also found that TRAP-positive mono- and multinucleated osteoclast lineage cells in the tumor nests. These results indicate that bone destruction induced by cancer metastasis is mainly caused by osteoclasts.

Several kinds of osteoclastogenic factors, such as PTHrP, prostaglandins, and interleukins, are produced by metastatic cancer cells in bone, which provide a microenvironment appropriate for the differentiation and activation of osteoclasts [1,5,13]. As previously described [13,14], our RT-PCR and immunohistochemical analyses also show that MDA-MB-231 cells produce PTHrP, one of the most responsible factors in the development of osteolytic bone metastases [1,13], but not RANKL. Histochemical and immunohistochemical examination demonstrated that ALP and RANKL-positive stromal cells were frequently adjacent to TRAP-positive mononuclear osteoclast precursor cells. Most importantly, immunoelectron microscopy

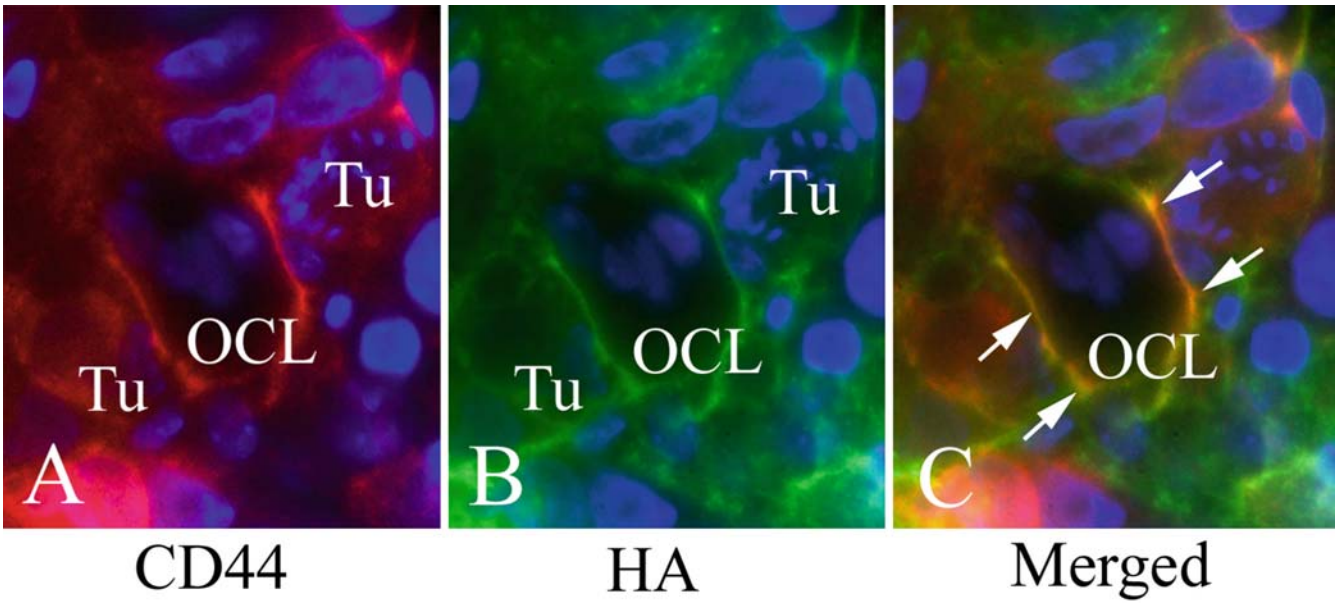

Fig. 4. Fluorescent micrographs indicating *CD44* and hyaluronan (*HA*). **A** Tumor cells (*Tu*) and a multinuclear osteoclast-like cell (*OCL*) in a tumor nest show immunoreactivity for CD44 (stained *red*). **B** HA-positive labeling (stained *green*) is detected along the tumor cells (*Tu*) and the osteoclast-like cell (*OCL*). **C** Colocalization of CD44 and HA (arrows) is seen in the contact region between the tumor cells and the osteoclast-like cell (OCL). ×1000

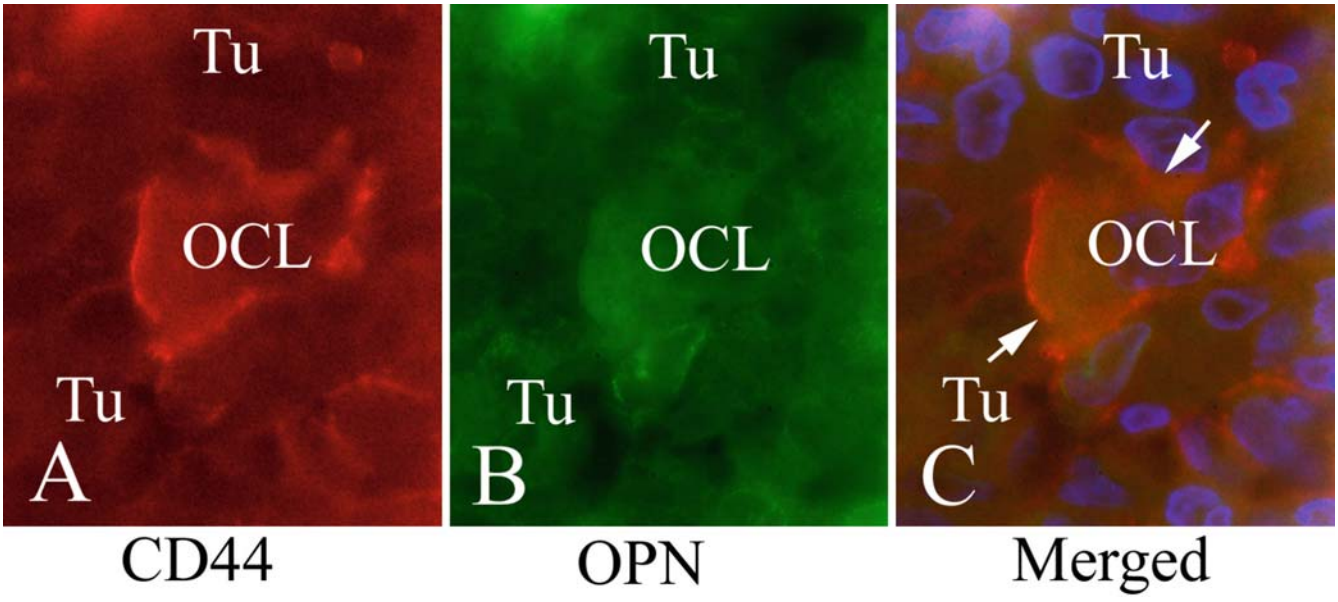

Fig. 5. Fluorescent micrographs indicating *CD44* and osteopontin (*OPN*). **A** Tumor cells (*Tu*) and a multinuclear osteoclast-like cell (*OCL*) in a tumor nest show immunoreactivity for CD44 (stained *red*). **B** OPN-positive labeling (stained *green*) is detected in the tumor cells (*Tu*) and extracellular matrices. **C** Colocalization of CD44 and OPN (*arrows*) is seen in the contact region between the tumor cells and the osteoclast-like cell (*OCL*). ×1000

revealed that those RANKL-positive stromal cells were in direct contact with osteoclast lineage cells. These results suggest that, also in metastatic bone diseases, the activation of RANKL-RANK signals mediated by the cell–cell interactions between bone marrow stromal cells and osteoclast precursor cells plays a critical role in osteoclast differentiation. The finding that MDA-MB-231 cells express PTHrP but not RANKL suggests that MDA-MB-231 cells induce bone destruction indirectly by upregulating RANKL expression in the stromal cells.

Cell–cell and cell–matrix interactions mediated by CAMs are critical for cancer metastasis [2]. They also play roles in osteoclast differentiation and activation [8–11,16,17]. Our study shows that CD44 was expressed on the plasma membranes of osteoclast-like cells and metastatic MDA-MB-231 cells colonized in bone. The ligands HA and OPN were also

found in the extracellular spaces in the tumor nests and were partially colocalized with CD44. As these molecules have been shown to positively regulate osteoclast differentiation and function [22–27], it is plausible that they act to facilitate bone destruction in bone metastases. In support of this notion, osteoclastogenesis and tumor growth in bone were suppressed in OPN-deficient mice [29]. It has been also demonstrated that HA increased RANKL expression in bone marrow stromal cells through CD44 [27]. Furthermore, Spessotto et al. proposed that the interactions of HA with CD44 expressed in osteoclastic cells hampers their migration [30]. These data together with our results showing the colocalization of CD44, HA, and OPN between cancer cells, bone marrow stromal cells, and osteoclast-like cells suggest that their interactions may hold osteoclast precursor cells and positively assist the RANKL-RANK-mediated cell signals, leading to enhanced osteoclastic bone destruction in bone metastases.

In conclusion, our results provide morphological evidence supporting that osteoclastogenic factors, including PTHrP, produced by the metastatic cancer cells upregulate RANKL expression in bone marrow stromal cells, which in turn stimulates osteoclast differentiation and function, thereby promoting osteoclastic bone destruction in the bone metastases. The results also suggest that the cell–matrix interactions between cancer cells, bone marrow stromal cells, and osteoclast precursor cells mediated by CD44, HA, and OPN may act to enhance osteoclastic bone destruction.

References

1. Mundy GR (2002) Metastasis to bone: causes, consequences and therapeutic opportunities. Nat Rev Cancer 2:584–593
2. Yoneda T, Hiraga T (2005) Crosstalk between cancer cells and bone microenvironment in bone metastasis. Biochem Biophys Res Commun 328:679–687
3. Boyde A, Maconnachie E, Reid SA, Delling G, Mundy GR (1986) Scanning electron microscopy in bone pathology: review of methods, potential and applications. Scanning Electron Microsc 4:1537–1554
4. Hiraga T, Tanaka S, Ikegame M, Koizumi M, Iguchi H, Nakajima T, Ozawa H (1998) Morphology of bone metastasis. Eur J Cancer 34:230–239
5. Hiraga T, Myoui A, Choi ME, Yoshikawa H, Yoneda T (2006) Stimulation of cyclooxygenase-2 expression by bone-derived transforming growth factor β enhances bone metastases in breast cancer. Cancer Res 66:2067–2073
6. Ito M, Amizuka N, Tanaka S, Funatsu-Ozawa Y, Kenmotsu S, Oda K, Nakajima T, Ozawa H (2003) Ultrastructural and cytobiological studies on possible interactions between PTHrP-secreting tumor cells, stromal cells, and bone cells. J Bone Miner Metab 21: 353–362
7. Shimamura T, Amizuka N, Li M, Freitas PH, White JH, Henderson JE, Shingaki S, Nakajima T, Ozawa H (2005) Histological observations on the microenvironment of osteolytic bone metastasis by breast carcinoma cell line. Biomed Res 26:159–172
8. Suda T, Takahashi N, Udagawa N, Jimi E, Gillespie MT, Martin TJ (1999) Modulation of osteoclast differentiation and function by the new members of the tumor necrosis factor receptor and ligand families. Endocr Rev 20:345–357
9. Hofbauer LC, Neubauer A, Heufelder AE (2001) Receptor activator of nuclear factor-kappaB ligand and osteoprotegerin: potential implications for the pathogenesis and treatment of malignant bone diseases. Cancer (Phila) 92:460–470
10. Roodman GD (2006) Regulation of osteoclast differentiation. Ann N Y Acad Sci 1068:100–109
11. Asagiri M, Takayanagi H (2007) The molecular understanding of osteoclast differentiation. Bone (NY) 40:251–264
12. Southby J, Kissin MW, Danks JA, Hayman JA, Moseley JM, Henderson MA, Bennett RC, Martin TJ (1990) Immunohistochemical localization of parathyroid hormone-related protein in human breast cancer. Cancer Res 50:7710–7716
13. Guise TA, Yin JJ, Taylor SD, Kumagai Y, Dallas M, Boyce BF, Yoneda T, Mundy GR (1996) Evidence for a causal role of parathyroid hormone-related protein in the pathogenesis of human breast cancer-mediated osteolysis. J Clin Invest 98:1544–1549
14. Thomas RJ, Guise TA, Yin JJ, Elliott J, Horwood NJ, Martin TJ, Gillespie MT (1999) Breast cancer cells interact with osteoblasts to support osteoclast formation. Endocrinology 140:4451–4458
15. Kitazawa S, Kitazawa R (2002) RANK ligand is a prerequisite for cancer-associated osteolytic lesions. J Pathol 198:228–236
16. McHugh KP, Shen Z, Crotti TN, Flannery MR, Fajardo R, Bierbaum BE, Goldring SR (2007) Role of cell-matrix interactions in osteoclast differentiation. Adv Exp Med Biol 602:107–111
17. Nakamura I, Cuong le T, Rodan SB, Rodan GA (2007) Involvement of $\alpha_v\beta_3$ integrins in osteoclast function. J Bone Miner Metab 25:337–344
18. Nakamura H, Kenmotsu S, Sakai H, Ozawa H (1995) Localization of CD44, the hyaluronate receptor, on the plasma membrane of osteocytes and osteoclasts in rat tibiae. Cell Tissue Res 280: 225–233
19. Draffin JE, McFarlane S, Hill A, Johnston PG, Waugh DJ (2004) CD44 potentiates the adherence of metastatic prostate and breast cancer cells to bone marrow endothelial cells. Cancer Res 64:5702–5711
20. Bajorath J (2000) Molecular organization, structural features, and ligand binding characteristics of CD44, a highly variable cell surface glycoprotein with multiple functions. Proteins 39:103–111
21. Turley EA, Noble PW, Bourguignon LY (2002) Signaling properties of hyaluronan receptors. J Biol Chem 277:4589–4592
22. Kania JR, Kehat-Stadler T, Kupfer SR (1997) CD44 antibodies inhibit osteoclast formation. J Bone Miner Res 12:1155–1164
23. de Vries TJ, Schoenmaker T, Beertsen W, van der Neut R, Everts V (2005) Effect of CD44 deficiency on in vitro and in vivo osteoclast formation (2005) J Cell Biochem 94:954–966
24. Ariyoshi W, Takahashi T, Kanno T, Ichimiya H, Takano H, Koseki T, Nishihara T (2005) Mechanisms involved in enhancement of osteoclast formation and function by low molecular weight hyaluronic acid. J Biol Chem 280:18967–18972
25. Rittking SR, Matsumoto HN, McKee MD, An XR, Novick KE, Kowalski AJ, Noda M, Denhardt DT (1998) Mice lacking osteopontin show normal development and bone structure but display altered osteoclast formation in vitro. J Bone Miner Res 13: 1101–1111
26. Chellaiah MA, Kizer N, Biswas R, Alvarez U, Strauss-Schoenberger J, Rifas L, Rittling SR, Denhardt DT, Hruska KA (2003) Osteopontin deficiency produces osteoclast dysfunction due to reduced CD44 surface expression. Mol Biol Cell 14:173–189
27. Cao JJ, Singleton PA, Majumdar S, Boudignon B, Burghardt A, Kurimoto P, Wronski TJ, Bourguignon LY, Halloran BP (2005) Hyaluronan increases RANKL expression in bone marrow stromal cells through CD44. J Bone Miner Res 20:30–40
28. Nakamura H, Kato R, Hirata A, Inoue M, Yamamoto T (2005) Localization of CD44 (hyaluronan receptor) and hyaluronan in rat mandibular condyle. J Histochem Cytochem 53:113–120
29. Ohyama Y, Nemoto H, Rittling S, Tsuji K, Amagasa T, Denhardt DT, Nifuji A, Noda M (2004) Osteopontin-deficiency suppresses growth of B16 melanoma cell implanted in bone and osteoclastogenesis in co-cultures. J Bone Miner Res 19:1706–1711
30. Spessotto P, Rossi FM, Degan M, Di Francia R, Perris R, Colombatti A, Gattei V (2002) Hyaluronan-CD44 interaction hampers migration of osteoclast-like cells by down-regulating MMP-9. J Cell Biol 158:1133–1144